Primordial nucleosynthesis *

L.J. van den Horn
Universiteit van Amsterdam

April 2, 2003

*Interacademiaal college 'Het vroege heelal', Universiteit Utrecht 2003

1 Introduction

The Standard Model of cosmology rests on three pillars of observational evidence, the expansion of the universe (Hubble 1929), the 3K background radiation (Penzias & Wilson 1965), and the cosmic abundances of the light elements (hydrogen, deuterium, helium, and lithium). While spanning some nine orders of magnitude, these abundances agree remarkably well with their theoretical predictions, and their dependence on the baryon/photon ratio allows for a rather precise determination of the baryon matter density in the universe. A major argument in support of primordial nucleosynthesis is that the average amount of helium in the universe (nearly 25% by mass) by far exceeds what could have been produced by stellar processes. The essentials of cosmological nucleosynthesis can be understood from the notion that at some point in the early history of the universe the neutron/proton ratio, before decreasing all too steeply with temperature, was 'frozen in'. Free neutrons were thus able to survive the cooling of the primeval plasma and were subsequently available for nuclear fusion. These neutrons nearly all end up in helium-4 which has the largest binding energy, through two possible chains

$$\begin{aligned} p + n &\rightarrow d + \gamma \\ d + d &\rightarrow {}^3He + n \\ &\text{or} \quad {}^3H + p \\ {}^3He + d &\rightarrow {}^4He + p \\ {}^3H + d &\rightarrow {}^4He + n \end{aligned}$$

Here d stands for the deuteron ${}^2H$. Beyond helium, a small amount of lithium can be formed through the reactions

$$\begin{aligned} {}^4He + {}^3H &\rightarrow {}^7Li + \gamma \\ {}^4He + {}^3He &\rightarrow {}^7Be + \gamma \\ {}^7Be + \gamma &\rightarrow {}^7Li + p \end{aligned}$$

Since the typical binding energies of the light nuclei are of order 1 MeV per nucleon (see Table), one would expect nucleosynthesis to take place following cooling of the universe down to this energy range. However, we will see that the huge radiation entropy of the universe (witness the smallness, $\eta \sim 10^{-10}$,

of the baryon/photon ratio) prevents nuclear fusion to get well under way until temperatures ~ 0.1 MeV prevail.

A	B_A (MeV)
^2H	2.22
^3H	6.92
^3He	7.72
^4He	28.3

The absence of stable nuclei with atomic number 5 and 8 which makes it impossible to form a nucleus out of $^4He + p$, the low number densities preventing the triple-alpha process by which carbon is formed in stars, and increasing suppression of nuclear reactions by the Coulomb barrier entail the end of the epoch of nucleosynthesis after ~ 10 minutes, leaving the universe as yet without a trace of heavy nuclei.

2 Particle and energy densities

The number and energy densities of particles in thermal equilibrium are given by the statistical expressions

$$n_i = \frac{g_i}{(2\pi\hbar)^3} \int \frac{4\pi p_i^2 dp_i}{\exp((\epsilon_i - \mu_i)/kT) \pm 1} \tag{2.1}$$

$$\rho_i = \frac{g_i}{(2\pi\hbar)^3} \int \frac{\epsilon_i \cdot 4\pi p_i^2 dp_i}{\exp((\epsilon_i - \mu_i)/kT) \pm 1} \tag{2.2}$$

Here g_i is the statistical weight, p_i the magnitude of the momentum, ϵ_i the energy, and μ_i the chemical potential of a particle of species i. In the integrand we recognize the Fermi-Dirac $(+)$ or the Bose-Einstein $(-)$ equilibrium distribution at temperature T. Particle energy and momentum are related through

$$\epsilon_i = (p_i^2 + m_i^2)^{1/2} \tag{2.3}$$

with m_i the mass of the particle (units such that the speed of light $c = 1$). The particles are in equilibrium (LTE) as long as their collision rates are sufficiently high, *i.e.*, faster than the cosmic expansion rate (see also below).

In the MeV range, the cosmic fluid is nearly entirely composed of relativistic particles, namely

• *Photons* ($g = 2, \mu = 0$)

$$n_\gamma = \frac{1}{\pi^2}\left(\frac{kT}{\hbar c}\right)^3 \int_0^\infty \frac{x^2 dx}{e^x - 1} = \frac{2\zeta(3)}{\pi^2}\left(\frac{kT}{\hbar c}\right)^3 \tag{2.4}$$

$$\rho_\gamma = \frac{1}{\pi^2}\frac{(kT)^4}{(\hbar c)^3}\int_0^\infty \frac{x^3 dx}{e^x - 1} \equiv aT^4 \tag{2.5}$$

with the radiation constant $a \equiv \pi^2 k^4/15(\hbar c)^3 \simeq 7.56 \times 10^{-15}\, erg\, cm^{-3} K^{-4}$. The factor $\zeta(3) \simeq 1.202$ arises from the Riemann zeta function. The constant c has here been made explicit.

• *Electrons* ($g = 2$)
With $\mu = 0$, the densities follow as

$$n_{e^-} = n_{e^+} = \pi^{-2} T^3 \int_0^\infty \frac{x^2 dx}{e^x + 1} = \pi^{-2} T^3 \cdot \frac{3}{2}\zeta(3) = \frac{3}{4} n_\gamma \tag{2.6}$$

$$\rho_{e^-} = \rho_{e^+} = \frac{7}{8}\rho_\gamma \tag{2.7}$$

• *Neutrinos* ($g = 1$)
Here $\mu = 0$ yields

$$n_\nu = n_{\bar{\nu}} = \frac{3}{8} n_\gamma \tag{2.8}$$

$$\rho_\nu = \rho_{\bar{\nu}} = \frac{7}{16}\rho_\gamma \tag{2.9}$$

The lepton chemical potentials have been assumed to vanish. For the electrons this is justified in view of the charge neutrality requirement; for the neutrinos the assumption holds to the extent that, like for electrons, particles and antiparticles are equally abundant.

In addition to these relativistic constituents, there is a trace of nonrelativistic free protons and neutrons, with number densities

$$n_N = 2\left(\frac{m_N kT}{2\pi\hbar^2}\right)^{3/2} e^{(\mu_N - m_N)/kT} \quad , \quad N = n, p \tag{2.10}$$

Accordingly, the (equilibrium) ratio of neutrons and protons is given by

$$\frac{n_n}{n_p} = \left(\frac{m_n}{m_p}\right)^{3/2} e^{(\mu_n - \mu_p - m_n + m_p)/kT} \approx e^{-\Delta m/kT} \quad , \tag{2.11}$$

with $\Delta m \equiv m_n - n_p \simeq 1.29$ MeV the mass difference. From this we see that $n_n/n_p \simeq 1$ for $kT \gg 1$ MeV, but this ratio is exponentially suppressed once the temperature drops below ~ 1 MeV.

The nucleons contribute negligibly to the total energy density which, given three different neutrino species, follows as

$$\rho = (1 + 2 \times \frac{7}{8} + 3 \times 2 \times \frac{7}{16}) a T^4 = \frac{43}{8} a T^4 \tag{2.12}$$

More generally, for relativistic bosons the thermal densities are

$$n_b = \frac{g_b}{2\pi^2} T^3 \cdot 2! \zeta(3) = \frac{g_b}{2} n_\gamma \tag{2.13}$$

$$\rho_b = \frac{g_b}{2\pi^2} T^4 \cdot 3! \zeta(4) = \frac{g_b}{2} \cdot a T^4 \tag{2.14}$$

while for fermions we have

$$n_f = \frac{g_f}{2\pi^2} T^3 \cdot \frac{3}{2} \zeta(3) = \frac{g_f}{2} \cdot \frac{3}{4} n_\gamma \tag{2.15}$$

$$\rho_f = \frac{g_f}{2\pi^2} T^4 \cdot \frac{7\pi^4}{120} = \frac{g_f}{2} \cdot \frac{7}{8} a T^4 \tag{2.16}$$

The total energy density in relativistic particles with temperature T can thus be written as

$$\rho = \frac{1}{2} \Sigma_{b,f} (g_b + \frac{7}{8} g_f) a T^4 \equiv \frac{1}{2} g_* a T^4 \tag{2.17}$$

This relation defines g_*, the effective number of degrees of freedom in relativistic particles[1]. For the photon-lepton plasma considered above, we have $g_* = 43/4$. Note that this parameter contains, in particular, the number of neutrino species.

In this early radiation dominated epoch, the energy density directly determines the expansion rate according to

$$H^2 = \frac{8\pi G}{3} \rho \tag{2.18}$$

since the curvature and vacuum terms in the Friedmann equation may be ignored. The Hubble expansion rate is defined as $H \equiv \dot{R}/R$, with $R(t)$ the cosmic scale factor. With the 'radiative' energy density (2.17) it follows that $H \propto g_*^{1/2} T^2$. From the conservation of energy of a comoving volume,

$$d(\rho R^3) + p dR^3 = 0 \tag{2.19}$$

[1] The definition can be extended to include different temperatures, see ref. [1].

with $p = \frac{1}{3}\rho$, we have $\rho \propto R^{-4}$, so that $R \propto t^{1/2}$, $H = \frac{1}{2}t^{-1}$. The age of the universe is thus given by $t_H = \frac{1}{2}H^{-1} \propto g_*^{-1/2}T^{-2}$. Numerically,

$$t_H \simeq 2.4 g_*^{-1/2}(kT[\mathrm{MeV}])^{-2} \quad \mathrm{sec} \tag{2.20}$$

From this one finds that the $(\gamma e^{\pm}\nu\bar{\nu})$ plasma with three neutrino flavors ($g_* = 43/4$) cools to 1 MeV in about three quarters of a second. Notice that additional neutrino flavors would speed up the expansion.

For a given value of g_*, *i.e.,* a fixed composition, the relation $\rho \propto T^4 \propto R^{-4}$ implies that the universe cools according to $T \propto R^{-1}$. This is basically a statement of entropy conservation, since the entropy density in radiation and relativistic particle pairs is

$$s = (\rho + p)/T \propto T^3 \tag{2.21}$$

In line with (2.17) one can write this relationship as

$$s = \frac{2}{3} g'_* a T^3 \tag{2.22}$$

where it is anticipated that g'_* is distinct from g_* if part of the entropy resides in decoupled species having a different temperature. As we will see in the next section, this is the case for neutrinos after the epoch of electron-positron annihilation.

3 Neutrino decoupling

Thermal coupling of the neutrinos is mediated through weak reactions such as

$$e^{\pm} + \nu \rightarrow e^{\pm} + \nu \quad , \quad e^{\pm} + \bar{\nu} \rightarrow e^{\pm} + \bar{\nu} \tag{3.23}$$

$$e^{\pm} \longleftrightarrow \nu\bar{\nu} \tag{3.24}$$

whose rates are typically proportional to T^5, so that they decrease much faster with T than the Hubble rate. As their rates fall below the expansion rate, these weak reactions 'freeze out', and neutrinos lose thermal contact with the other constituents. The decoupled neutrinos thereupon form a freely expanding inert thermal background of particles, whose temperature is 'redshifted' ($T_\nu \propto 1/R$) by the cosmic expansion.

Since the reaction rates depend steeply on temperature, decoupling occurs in a fairly restricted temperature range around ~ 1 MeV. Consider the weak reaction rates

$$\Gamma_w = n_\ell \langle \sigma_w c \rangle \tag{3.25}$$

where the brackets indicate an appropriate thermal average. We may estimate this quantity using the typical number density of leptons

$$n_\ell \approx \left(\frac{kT}{\hbar c}\right)^3 \tag{3.26}$$

and the 'thermal' weak cross section

$$\sigma_w = G_F^2 \frac{(kT)^2}{(\hbar c)^4} \tag{3.27}$$

with $G_F \simeq 1.4 \times 10^{-49}\, erg\, cm^3$ the Fermi coupling constant. Comparing Γ_w to the expansion rate H, using the value $g_* = 43/4$, we then find that the reaction and expansion rates are equal at $kT \approx 2.3$ MeV.

One consequence of neutrino decoupling is that when electron-positron pairs annihilate at temperatures corresponding to the electron mass, $m_e \simeq 0.51$ MeV, the annihilation is into the photon channel only. This entails a change of composition, accounted for by the effective number of relativistic degrees of freedom. The entropy in $e^\pm$ pairs is transferred to the photons, which effectively implies heating of the latter. Since the entropy of the decoupled neutrinos is separately conserved, entropy conservation implies that the final photon entropy density equals that of the pre-annihilation $(\gamma e^\pm)$ fluid, so that the higher temperature T' is given by $T'^3 = (1+7/4)T^3$. It follows that the photon temperature is raised by 40% due to the $e^\pm$ annihilation

$$T'/T = (11/4)^{1/3} \simeq 1.4 \tag{3.28}$$

Since the neutrinos remain unaffected, this is from now on also the ratio T_γ/T_ν, where T_ν is the temperature of the neutrino background, while the photon temperature T_γ represents the temperature of the post-annihilation $(\gamma e^- pn)$ plasma. As long as the neutrinos are relativistic, both T_γ and T_ν are redshifted as $1/R$, so their ratio remains constant. This argument predicts that 'today', in addition to the 2.73 K photon background, there would be an undetected 1.96 K background of light neutrinos. This temperature loses its strict meaning if the neutrinos would not be practically massless. Note however, that the neutrino *number* densities would still be given by

$$n_{\nu\bar{\nu}} = \frac{4}{11} \cdot \frac{3}{4} n_\gamma = \frac{3}{11} n_\gamma \tag{3.29}$$

for each flavor. Since the number density of background photons is about 411 per cm^3, as measured directly from their temperature of 2.73 K, it follows that the neutrino background contains per cm^3 about 112 neutrinos

and antineutrinos of each flavor. As has been realized for many years, from this knowledge a cosmological bound can be set on the neutrino mass ¶[2].

The different photon and neutrino temperatures lead to different values of g_* and g'_*, the energy and entropy degrees of freedom. After $e^{\pm}$ annihilation we have

$$g_* = 2 + 3 \times 2 \times \frac{7}{8} \times \left(\frac{4}{11}\right)^{4/3} = 3.36 \tag{3.30}$$

$$g'_* = 2 + 3 \times 2 \times \frac{7}{8} \times \frac{4}{11} = 3.91 \tag{3.31}$$

since energy density scales as T^4, while entropy density scales as T^3.

Neutrino decoupling also has profound consequences for the neutron-proton ratio, since the equilibrium value

$$n_n/n_p = e^{-\Delta m/kT} = e^{-1.29\mathrm{MeV}/kT} \tag{3.32}$$

is maintained through the weak reactions

$$\nu_e + n \longleftrightarrow p + e^- \quad , \quad \bar{\nu}_e + p \longleftrightarrow n + e^+ \tag{3.33}$$

These neutrino absorptions, which interconvert the nucleons, freeze out as neutrinos decouple. As a result the n/p ratio will cease to follow the exponential decline, and is 'frozen in' at a value corresponding to the decoupling temperature. The value of 2.3 MeV for the latter, as estimated above, would result in $n_n/n_p \simeq 0.57$ at freeze out, or individual concentrations $X_n \simeq 0.36$ and $X_p \simeq 0.64$. Since the relative mass difference is negligibly small, these values may be taken as mass concentrations as well as free number fractions.

The fraction of free neutrons is the primary quantity determining the helium yield. After freeze out of the reactions (3.33), the neutron fraction can still decrease somewhat further through free neutron decay

$$n \longrightarrow p + e^- + \bar{\nu}_e \tag{3.34}$$

according to which

$$X_n(t) = X_n^* e^{-t/\tau_n} \tag{3.35}$$

Here X_n^* denotes the neutron fraction at freeze out, and $\tau_n \simeq 887\,s$ is the decay time. The final fraction of neutrons available for nucleosynthesis is thus fixed by time available for decay. With nuclear fusion occurring around $kT \sim 0.1$ MeV, this time span is approximately 130 seconds, lowering the

[2]Topic may be selected for examination paper.

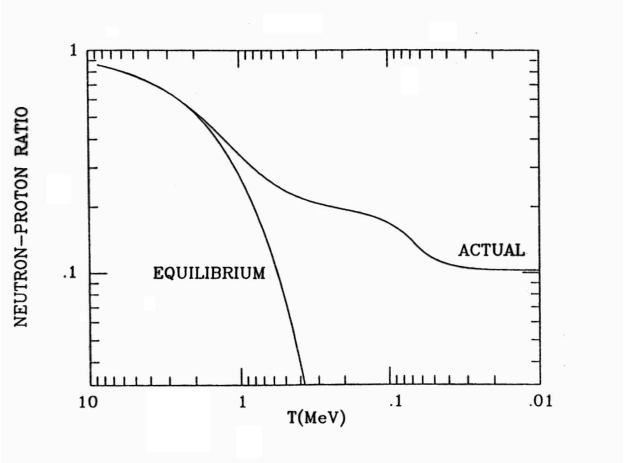

Figure 1: Actual and equilibrium behavior of the neutron/proton ratio. (Figure adapted from [1].)

final fraction to $X_n \simeq 0.31$. As nearly all these neutrons will end up in ^4He, a helium abundance by mass

$$X_\alpha = \frac{4 \times \frac{1}{2} n_n}{n_n + n_p} \simeq 0.62 \tag{3.36}$$

would eventually be produced.

This figure is way too high: the actually observed abundance is somewhat less than 25%. If this percentage is taken as an upper limit, the final neutron/proton ratio should clearly not exceed the value 1/7. Our present discrepancy is due mainly to the fact that the final neutron fraction depends sensitively on the neutrino decoupling temperature which we have rather crudely estimated. The cross section for the reactions (3.33) is more appropriately represented by the characteristic absorption cross section

$$\sigma_a = (1 + 3g_a^2) G_F^2 (kT)^2 / (\hbar c)^4 \tag{3.37}$$

where $g_a \simeq 1.26$ is the axial coupling constant. This enhances our previous estimate for the reaction rates, giving a correspondingly lower freeze-out temperature $kT \approx 1.3$ MeV and final fractions $X_n = 0.23$ and $X_\alpha = 0.46$, respectively. These values are still too high, compared not only to the observations, but as well to detailed numerical calculations of the helium and

other light element abundances involving a full reaction network[3]. The essential physics of cosmological helium production is nonetheless contained in the arguments presented. In the next section we address the other light elements.

4 Nuclear abundances

The equilibrium number densities of the nuclear species are given by expressions similar to the nucleonic densities (2.10)

$$n_A = g_A \left(\frac{m_A T}{2\pi}\right)^{3/2} e^{(\mu_A - m_A)/T} \tag{4.38}$$

Here $c, \hbar$ and k have been set equal to 1. The species are labeled by their atomic number A. In chemical reaction equilibrium, the chemical potential is given by

$$\mu_A = Z\mu_p + (A - Z)\mu_n \tag{4.39}$$

where Z is the proton number of the nucleus. With the help of (2.10) we can then express n_A in terms of the nucleon number densities

$$n_A = g_A A^{3/2} 2^{-A} (2\pi/m_N T)^{3(A-1)/2} n_p^Z n_n^{A-Z} \, e^{B_A/T} \tag{4.40}$$

where

$$B_A \equiv Z m_p + (A - Z) m_n - m_A \tag{4.41}$$

is the binding energy of nucleus A (see the table in section 1). The mass fraction of nuclei is

$$X_A \equiv A n_A / n_N \tag{4.42}$$

where n_N is now defined as the *total* (conserved) nucleon density. The latter is nothing else than the baryon density of the universe, so that $n_N = \eta n_\gamma$, and the nuclear mass fractions follow as

$$\begin{aligned} X_A &= g_A \pi^{-(A-1)/2} \zeta(3)^{A-1} A^{5/2} 2^{(3A-5)/2} (T/m_N)^{3(A-1)/2} \\ &\quad \times \eta^{A-1} X_p^Z X_n^{A-Z} \exp(B_A/T) \end{aligned} \tag{4.43}$$

Noting in particular the dependence on the baryon/photon ratio η, we may anticipate quite low equilibrium abundances until T has dropped significantly. For example, in spite of the high binding energy of ^4He, its mass concentration

$$X_\alpha \simeq 113 (T/m_N)^{9/2} \eta^3 X_p^2 X_n^2 \, e^{28.3\, MeV/T} \tag{4.44}$$

[3] For a rate calculation leading to the 'correct' freeze out temperature ~ 0.8 MeV, see ref. [2].

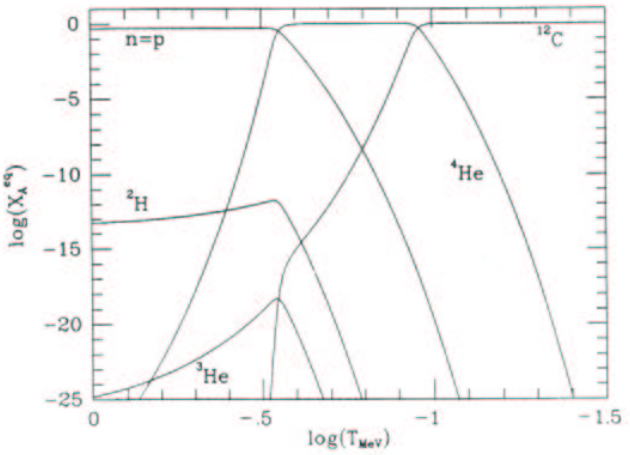

Figure 2: Equilibrium abundances as calculated from eq. (4.43). For simplicity the n and p fractions were taken to be equal. (Figure taken from [1].)

is still completely negligible ($\sim 10^{-28}$) at $T \sim 1$ MeV. In Fig.2 it is seen that X_α becomes substantial only at temperatures ~ 0.3 MeV.

Fig. 3 shows the development of nucleosynthesis by way of the calculated abundances relative to hydrogen. The actual abundances are different from the equilibrium values, because chemical equilibrium is not maintained. The (low) equilibrium abundance of deuterium, for example, constitutes the balance of deuterium production and its photodissociation. The latter process becomes inefficient below ~ 0.1 MeV, so that the actual abundance can rise to values of order 10^{-5} to 10^{-3}, and give a boost to helium production.

The predicted final abundances depend on a number of input parameters, notably the neutron half-life, number of neutrino flavors, and the adopted baryon/photon ratio. The dependence on the latter is shown in Fig. 4, which also illustrates the sensitivity of the helium-4 yield to the number of neutrino flavors. As remarked in section 2, additional neutrino flavors add to the total energy density and accelerate the expansion. As a consequence, more neutrons would remain available for helium production. This fact is exploited to constrain the number of neutrino flavors through the cosmological helium abundance ¶[4]. In a similar way, from the η-dependence of the predicted abundances one may impose restrictions on the present baryonic

[4]Topic may be selected for exam paper.

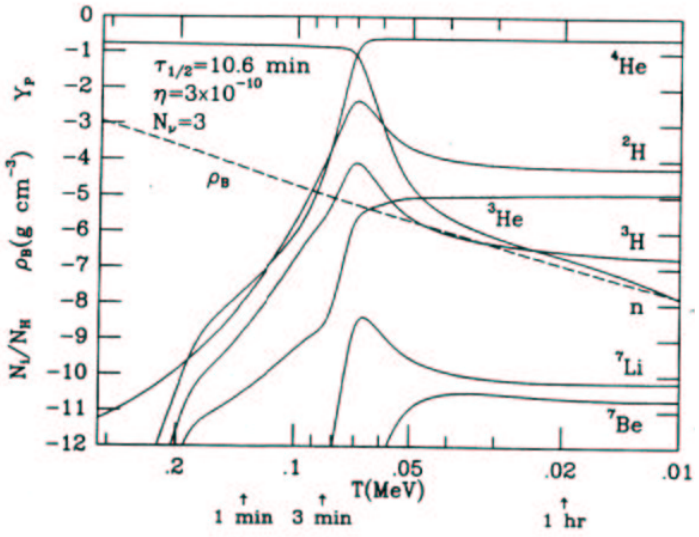

Figure 3: Development of primordial nucleosynthesis. The dashed line is the baryon mass density, and the solid lines are the mass fraction of helium-4 and the number fractions relative to hydrogen of the other light elements. (Figure taken from [1].)

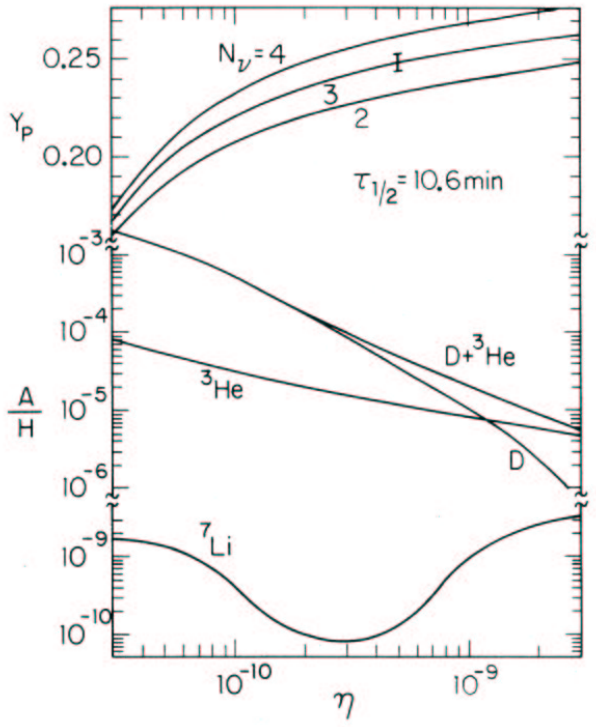

Figure 4: Predicted primordial abundances of the light elements. The fraction Y_p of ^4He is indicated for $N_\nu = 2, 3, 4$ light neutrino species. Comparison with the observational data defines a consistent range for the baryon/photon ratio η. (Figure taken from [1].)

matter density. Here the relative deuterium abundance is a particularly powerful probe, in view of its sensitivity to η. While a higher value of η results in the production of more helium, this will cause more depletion of the intermediate products. Finally, the so-called trough in the abundance of ^7Li is due to the existence of two different production channels (*cf.* section 1). Remarkably, this makes lithium a good probe of the baryon density, as its observed abundance is within the range of the trough.

5 Observations

Astronomical observations ¶[5] provide the test of nucleosynthesis predictions. The observed helium and lithium abundances in low metallicity extragalactic HII regions and old ('metal-poor') halo stars are extrapolated to zero metallicity to infer primordial values.

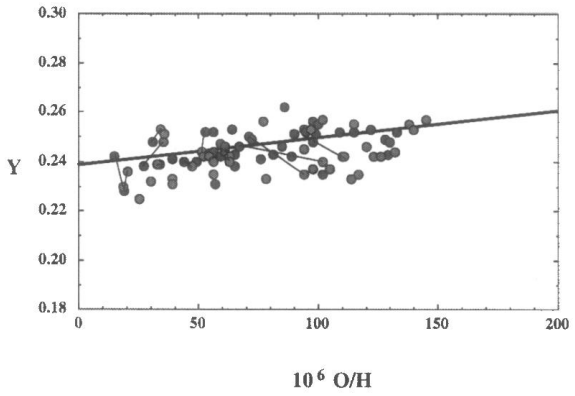

Figure 5: Helium and oxygen abundances observed in extragalactic HII regions. Lines connect the same regions observed by different groups. The primordial helium abundance is inferred from the extrapolation to zero metallicity. (Figure taken from [3].)

Lithium data are found to exhibit 'plateaus' indicative of the primordial abundance.

Deuterium, apart from the solar system and the Galaxy, has recently also been measured in some intergalactic clouds at high redshift which are so called Lyman-α absorbers of the light of distant quasars. These measurements should reflect the primordial abundance, or at any rate a lower bound to it, since deuterium is easily destroyed.

An especially strong test consists in the simultaneous agreement of predicted and observed values for all four light elements combined. Consistency is obtained for a fairly narrow range of values of η, providing a much more precise determination of the baryon matter density in the universe than traditional observational estimates.

Fig. 7 displays the theoretical predictions of extensive nucleosynthesis calculations [4] as a function of the baryon/photon ratio together, with the

[5]Topic may be selected for exam paper

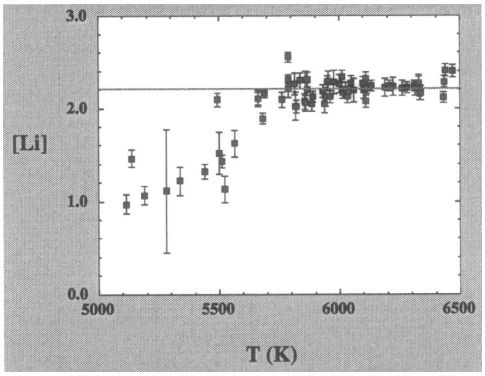

Figure 6: Lithium abundances (logarithm relative to solar) in low metallicity halo stars. (Figure taken from [3].)

observations and the associated theoretical and observational uncertainties. Since the deuterium observations are not unanimous, one may distinguish two data sets, a *low* and a *high* deuterium range, which both appear to meet the concordance requirements.

'low D'	Predicted	Observed
η	$(4.2 - 6.3) \times 10^{-10}$	
D/H	$(2.9 - 4.0) \times 10^{-5}$	input
Li/H	$(1.3 - 6.3) \times 10^{-10}$	$(1.3 - 2.0) \times 10^{-10}$
Y	0.244 - 0.250	0.228 - 0.248

'high D'	Predicted	Observed
η	$(1.2 - 2.8) \times 10^{-10}$	
D/H	$(10 - 30) \times 10^{-5}$	input
Li/H	$(0.8 - 5.0) \times 10^{-10}$	$(1.3 - 2.0) \times 10^{-10}$
Y	0.225 - 0.241	0.228 - 0.248

In these tables, as in the figures, Y stands for the helium-4 abundance previously denoted by X_α. In both cases a significant overlap exists, for helium as well as lithium, in the predicted and observed ranges. Therefore, these predictions alone do not favor either the low or the high deuterium data. On the other hand, the range of η corresponding to the low data set is indicated as well by new measurements involving the cosmic background radiation and data from Type Ia supernovae. Such new observational data track the baryon density practically from big bang to present [5]. In this

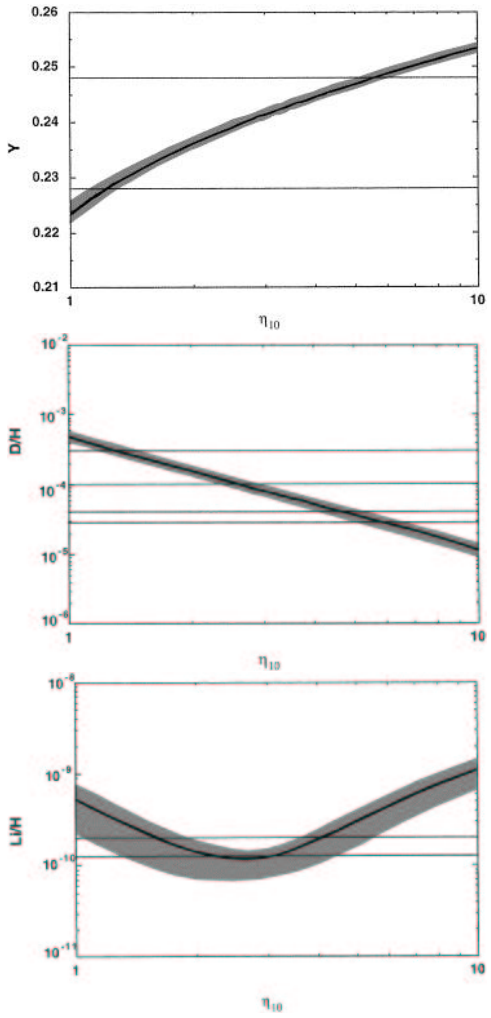

Figure 7: Light element abundances and their theoretical (2σ) and observational uncertainties. (Figures taken from [4].)

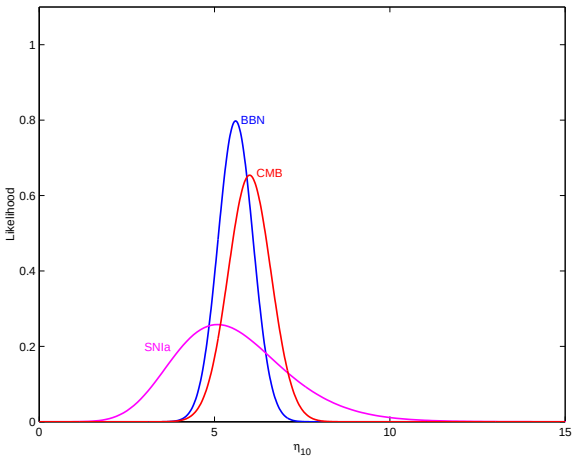

Figure 8: Likelihood distributions (normalized to equal areas under the curves) for η as derived from nucleosynthesis (BBN), the cosmic microwave background (CMB), and for the present universe (SNIa). (Figure taken from [5].)

perspective, the agreement of the distributions in Fig. 8 indeed becomes all the more striking!

References

[1] E.W. Kolb & M.S. Turner, *The Early Universe*, Addison-Wesley Publ. Company (1993), ch.4.

[2] V. Mukhanov, *Nucleosynthesis without a computer*, astro-ph/030373 v1 (March 2003)

[3] L. van Andel, *Cosmological nucleosynthesis*, MSc thesis, ITF-UvA (2002)

[4] K.A. Olive, G. Steigman, T.P Walker, *Primordial nucleosynthesis: theory and observations*, Phys. Rep. **333** (2000) 389-407.

[5] G. Steigman, *The baryon density through the (cosmological) ages*, astro-ph/0202187 v1, (Feb. 2002).

Appendix

Observations

Primordial abundances are *inferred* from data!

^4He : Optical recombination lines in low Z extragalactic H II regions, extrapolation to $Z = 0$.

Large data set $\rightarrow$ small statistical errors, e.g.,

40 low Z regions $\rightarrow Y = 0.234 \pm 0.003$

45 low Z regions $\rightarrow Y = 0.244 \pm 0.002$

Corrections for systematic errors, e.g.

- neutral helium
- interstellar absorption
- collisional excitation

Many precise measurements with quite different results!

$$\boxed{95\% \text{ range : } Y = 0.228 - 0.248}$$

^7Li : Absorption spectra of low mass, very low Z Pop II halo stars

Larga data set, abundances define 'plateau' with little intrinsic dispersion

Observed range consistent with 'lithium valley'

^2D : 'baryometer'

Solar system & Galaxy: H I regions, resonant UV absorption from ground state (Lyman series)

$$\text{D/H} \sim 1.5 \times 10^{-5}$$

$$\text{Jupiter: } \sim 2.6 \times 10^{-5}$$

High z, low Z nearly primordial regions (Ly-α clouds), background QSO

$$\text{D/H} = 2.9 \text{ - } 4.0 \times 10^{-5}$$

'anomalous' high D : $\sim 20 \times 10^{-5}$ for $z = 0.701$ system